Wolfgang E. Nagel
Dietmar H. Kröner
Michael M. Resch *Editors*

High Performance Computing in Science and Engineering ’16

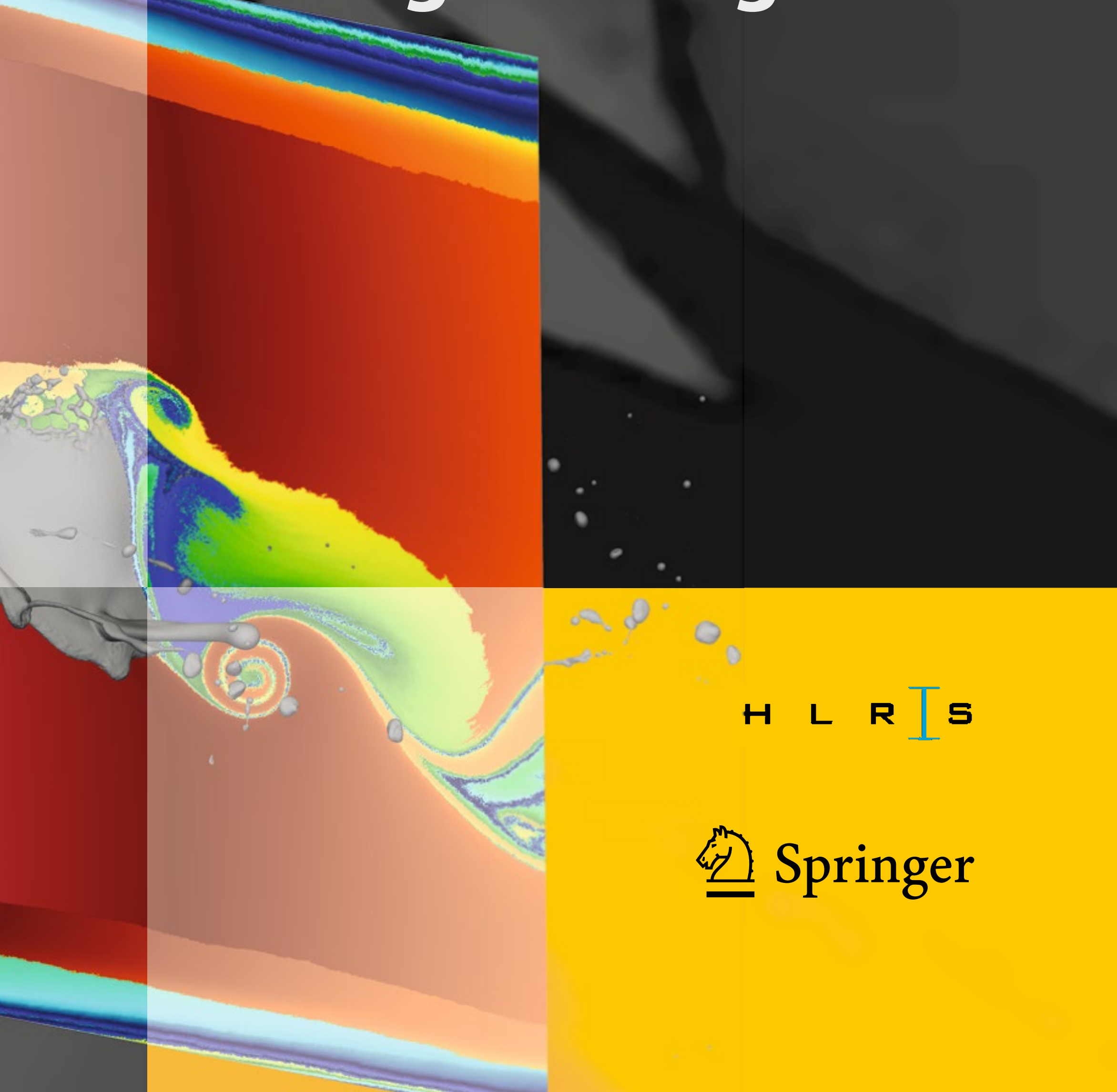

HLRS

Springer

High Performance Computing in Science and Engineering ’16

Wolfgang E. Nagel • Dietmar H. Kröner •
Michael M. Resch
Editors

High Performance Computing in Science and Engineering ’16

Transactions of the High Performance Computing Center, Stuttgart (HLRS) 2016

Springer

Editors
Wolfgang E. Nagel
Zentrum für Informationsdienste
und Hochleistungsrechnen (ZIH)
Technische Universität Dresden
Dresden
Germany

Dietmar H. Kröner
Abteilung für Angewandte Mathematik
Universität Freiburg
Freiburg
Germany

Michael M. Resch
Höchstleistungsrechenzentrum
Stuttgart (HLRS)
Universität Stuttgart
Stuttgart
Germany

Front cover figure: Bag breakup event during the air-assisted atomization of a liquid fuel. The air flow field is colored by particle IDs which depend on the creation time and their respective release position at the inlet. Details can be found in “Smoothed Particle Hydrodynamics for Numerical Predictions of Primary Atomization”, by S. Braun, R. Koch and H.-J. Bauer, Institut für Thermische Strömungsmaschinen (ITS), Karlsruher Institut für Technologie (KIT), Karlsruhe, Germany on page 321ff.

ISBN 978-3-319-47065-8 ISBN 978-3-319-47066-5 (eBook)
DOI 10.1007/978-3-319-47066-5

Library of Congress Control Number: 2016963434

Mathematics Subject Classification (2010): 65Cxx, 65C99, 68U20

Printed on acid-free paper

This Springer imprint is published by Springer Nature
The registered company is Springer International Publishing AG
The registered company address is: Gewerbestrasse 11, 6330 Cham, Switzerland

Contents

Part I Physics

The Illustris++ Project: The Next Generation of Cosmological Hydrodynamical Simulations of Galaxy Formation 5
Volker Springel, Annalisa Pillepich, Rainer Weinberger, Rüdiger Pakmor, Lars Hernquist, Dylan Nelson, Shy Genel, Mark Vogelsberger, Federico Marinacci, Jill Naiman, and Paul Torrey

Hydrangea: Simulating a Representative Population of Massive Galaxy Clusters 21
Yannick M. Bahé, for the C-EAGLE collaboration

PAMOP Project: Computations in Support of Experiments and Astrophysical Applications 33
B.M. McLaughlin, C.P. Ballance, M.S. Pindzola, P.C. Stancil, S. Schippers, and A. Müller

Estimation of Nucleation Barriers from Simulations of Crystal Nuclei Surrounded by Fluid in Equilibrium 49
Antonia Statt, Peter Koß, Peter Virnau, and Kurt Binder

The Internal Dynamics and Early Adsorption Stages of Fibrinogen Investigated by Molecular Dynamics Simulations 61
Stephan Köhler, Friederike Schmid, and Giovanni Settanni

Vorticity, Variance, and the Vigor of Many-Body Phenomena in Ultracold Quantum Systems: MCTDHB and MCTDH-X 79
Ofir E. Alon, Raphael Beinke, Lorenz S. Cederbaum, Matthew J. Edmonds, Elke Fasshauer, Mark A. Kasevich, Shachar Klaiman, Axel U.J. Lode, Nick G. Parker, Kaspar Sakmann, Marios C. Tsatsos, and Alexej I. Streltsov

Nucleon Observables as Probes for Physics Beyond the Standard Model 97
Constantia Alexandrou, Karl Jansen, Giannis Koutsou, and Carsten Urbach

Numerical Evaluation of Multi-loop Feynman Integrals 107
Peter Marquard and Matthias Steinhauser

Part II Molecules, Interfaces, and Solids

Mechanochemistry of Ring-Opening Reactions: From Cyclopropane in the Gas Phase to Thiotic Acid on Gold in the Liquid Phase 117
Martin Zoloff Michoff, Miriam Wollenhaupt, and Dominik Marx

Microscopic Insights into the Fluorite/Water Interfaces from Vibrational Sum Frequency Generation Spectroscopy 131
Rémi Khatib and Marialore Sulpizi

Growth, Structural and Electronic Properties of Functional Semiconductors Studied by First Principles 145
Andreas Stegmüller, Phil Rosenow, Lisa Pecher, Nikolay Zaitsev, and Ralf Tonner

Submonolayer Rare Earth Silicide Thin Films on the Si(111) Surface 163
S. Sanna, C. Dues, U. Gerstmann, E. Rauls, D. Nozaki, A. Riefer, M. Landmann, M. Rohrmüller, N.J. Vollmers, R. Hölscher, A. Lücke, C. Braun, S. Neufeld, K. Holtgrewe, and W.G. Schmidt

Computational Analysis of Li Diffusion in NZP-Type Materials by Atomistic Simulation and Compositional Screening 177
Daniel Mutter, Britta Lang, Benedikt Ziebarth, Daniel Urban, and Christian Elsässer

Molecular Dynamics Simulations of Silicon: The Influence of Electron-Temperature Dependent Interactions 189
Alexander Kiselev, Johannes Roth, and Hans-Rainer Trebin

Non-linear Quantum Transport in Interacting Nanostructures 203
Benedikt Schoenauer and Peter Schmitteckert

Part III Reactive Flows

A DNS Analysis of the Correlation of Heat Release Rate with Chemiluminescence Emissions in Turbulent Combustion 229
Feichi Zhang, Thorsten Zirwes, Peter Habisreuther, and Henning Bockhorn

Direct Numerical Simulation of Non-premixed Syngas Combustion Using OpenFOAM 245
Son Vo, Andreas Kronenburg, Oliver T. Stein, and Evatt R. Hawkes

Numerical Simulations of Rocket Combustion Chambers with Supercritical Injection 259
Martin Seidl, Roman Keller, Peter Gerlinger, and Manfred Aigner

Two-Zone Fluidized Bed Reactors for Butadiene Production: A Multiphysical Approach with Solver Coupling for Supercomputing Application 269
Matthias Hettel, Jordan A. Denev, and Olaf Deutschmann

Part IV Computational Fluid Dynamics

High-Pressure Real-Gas Jet and Throttle Flow as a Simplified Gas Injector Model Using a Discontinuous Galerkin Method 289
Fabian Hempert, Sebastian Boblest, Malte Hoffmann, Philipp Offenhäuser, Filip Sadlo, Colin W. Glass, Claus-Dieter Munz, Thomas Ertl, and Uwe Iben

Modeling of the Deformation Dynamics of Single and Twin Fluid Droplets Exposed to Aerodynamic Loads 301
Lars Wieth, Samuel Braun, Geoffroy Chaussonnet, Thilo F. Dauch, Marc Keller, Corina Höfler, Rainer Koch, and Hans-Jörg Bauer

Smoothed Particle Hydrodynamics for Numerical Predictions of Primary Atomization 321
Samuel Braun, Rainer Koch, and Hans-Jörg Bauer

Towards Solving Fluid Flow Domain Identification Problems with Adjoint Lattice Boltzmann Methods 337
Mathias J. Krause, Benjamin Förster, Albert Mink, and Hermann Nirschl

Investigation on Air Entrapment in Paint Drops Under Impact onto Dry Solid Surfaces 355
Qiaoyan Ye and Oliver Tiedje

Numerical Study of the Impact of Praestol® Droplets on Solid Walls 375
Martin Reitzle, Norbert Roth, and Bernhard Weigand

Turbulent Skin-Friction Drag Reduction at High Reynolds Numbers 389
Davide Gatti

Control of Spatially Developing Turbulent Boundary Layers for Skin Friction Drag Reduction 399
Alexander Stroh

Scalability of OpenFOAM with Large Eddy Simulations and DNS on High-Performance Systems 413
Gabriel Axtmann and Ulrich Rist

Numerical Simulation of Subsonic and Supersonic Impinging Jets II 425
Robert Wilke and Jörn Sesterhenn

Aeroacoustic Simulations of Ducted Axial Fan and Helicopter Engine Nozzle Flows 443
Alexej Pogorelov, Mehmet Onur Cetin, Seyed Mohsen Alavi Moghadam, Matthias Meinke, and Wolfgang Schröder

Adding Hybrid Mesh Capability to a CFD-Solver for Helicopter Flows 461
Ulrich Kowarsch, Timo Hofmann, Manuel Keßler, and Ewald Krämer

Direct Numerical Simulation of Heated Pipe Flow with Strong Property Variation 473
Xu Chu, Eckart Laurien, and Sandeep Pandey

CFD Analysis of Fast Transition from Pump Mode to Generating Mode in a Reversible Pump Turbine 487
Christine Stens and Stefan Riedelbauch

Scale Resolving Flow Simulations of a Francis Turbine Using Highly Parallel CFD Simulations 499
Timo Krappel and Stefan Riedelbauch

CFD Simulations of Thermal-Hydraulic Flows in a Model Containment: Phase Change Model and Verification of Grid Convergence 511
Abdennaceur Mansour, Christian Kaltenbach, and Eckart Laurien

Simulations of Unsteady Aerodynamic Effects on Innovative Wind Turbine Concepts 529
Annette Fischer, Levin Klein, Thorsten Lutz, and Ewald Krämer

Part V Transport and Climate

Simulation of the Rain Belt of the West African Monsoon (WAM) in High Resolution CCLM Simulation 547
Diarra Dieng, Gerhard Smiatek, Dominikus Heinzeller, and Harald Kunstmann

Anthropogenic Aerosol Emissions and Rainfall Decline in South-West Australia 559
Dominikus Heinzeller, Wolfgang Junkermann, and Harald Kunstmann

High-Resolution Climate Projections Using the WRF Model on the HLRS 577
Viktoria Mohr, Kirsten Warrach-Sagi, Thomas Schwitalla, Hans-Stefan Bauer, and Volker Wulfmeyer

Biogeophysical Impacts of Land Surface on Regional Climate in Central Vietnam 589
Ngoc Bich Phuong Nguyen, Harald Kunstmann, Patrick Laux, and Johannes Cullmann

Reducing the Uncertainties of Climate Projections: High-Resolution Climate Modeling of Aerosol and Climate Interactions on the Regional Scale Using COSMO-ART: Interaction of Mineral Dust with Atmospheric Radiation over West-Africa 601
Bernhard Vogel, Hans-Juergen Panitz, and Heike Vogel

Part VI Miscellaneous Topics

Molecular Simulation Study of Transport Properties for 20 Binary Liquid Mixtures and New Force Fields for Benzene, Toluene and CCl_4 613
Gabriela Guevara-Carrion, Tatjana Janzen, Y. Mauricio Muñoz-Muñoz, and Jadran Vrabec

Large-Scale Phase-Field Simulations of Directional Solidified Ternary Eutectics Using High-Performance Computing 635
J. Hötzer, M. Kellner, P. Steinmetz, J. Dietze, and B. Nestler

Seismic Applications of Full Waveform Inversion 647
A. Kurzmann, L. Gaßner, N. Thiel, M. Kunert, R. Shigapov, F. Wittkamp, T. Bohlen, and T. Metz

A Massively Parallel Multigrid Method with Level Dependent Smoothers for Problems with High Anisotropies 667
Sebastian Reiter, Andreas Vogel, Arne Nägel, and Gabriel Wittum

Part I
Physics

Peter Nielaba

In this section, eight physics projects are described, which achieved important scientific results by using the CRAY XC40 (Hornet and Hazel Hen) of the HLRS. Fascinating new results are being presented in the following pages on astrophysical systems (simulations of galaxy formation, of massive galaxy clusters, and of photodissociation), soft matter systems (simulations of nucleation in colloidal systems and of dynamics and adsorption of fibrinogen), many body quantum systems (simulations of ultracold quantum systems) and elementary particle systems (simulations of nucleon observables and of the anomalous magnetic moment of the muon).

The studies of the astrophysical systems have focused on the galaxy formation, massive galaxy clusters, and on photodissociation of certain molecules.

V. Springel, A. Pillepich, R. Weinberger, R. Pakmor, L. Hernquist, J. Naiman, D. Nelson, M. Vogelsberger, and F. Marinacci from Heidelberg (V.S., A.P., R.W., R.P.), Cambridge USA (L.H., J.N., M.V., F.M.) and Garching (D.N.), in their project GCS-ILLU present results from a new generation of hydrodynamical simulations ("Illustris++" project, AREPO code), including new black hole physics and chemical enrichment models, using more accurate techniques and an enlarged dynamical range. The authors reproduced the appearance of a red sequence of galaxies, quenched by accreting supermassive black holes and computed disk galaxies populations with properties closely matching observational data. In addition, the authors predicted magnetic field amplifications through small-scale dynamo processes for galaxies of different sizes and types.

Yannick M. Bahé and the C-EAGLE collaboration from Garching used in their HLRS project GCS-HYDA the GADGET-3 code to simulate 25 galaxy clusters with high resolution ("Hydrangea" project). By the ongoing data analysis new insights

P. Nielaba (✉)
Fachbereich Physik, Universität Konstanz, 78457 Konstanz, Germany
e-mail: peter.nielaba@uni-konstanz.de

into the physics of galaxy formation in an extreme environment and on the growth of the massive haloes, in which cluster galaxies are embedded, are achieved.

B M McLaughlin, C P Ballance, M S Pindzola, P C Stancil, S Schippers and A Müller from the Universities of Belfast (B.M.M., C.P.B.), Auburn (M.S.P.), Georgia (P.C.S.), and Giessen (S.S., A.M.) investigated in their project *PAMOP* atomic, molecular and optical collisions on petaflop machines in order to support measurements at synchrotron radiation facilities and to study photodissociation effects for astrophysical applications. The Schrödinger and Dirac equations have been solved with the R-matrix or R-matrix with pseudo-states approach, and the time dependent close-coupling method has been used. Various systems and phenomena have been investigated, ranging from X-ray and inner-shell photoionization in atomic oxygen and argon ions, as well as in tungsten ions, the single-photon double ionization in helium, to the photodissociation in SH^+.

The studies of the soft matter systems have focused on nucleation barriers in colloidal systems and on the dynamics and adsorption of fibrinogen.

A. Statt, P. Koß, P. Virnau and K. Binder from the University of Mainz present in their project *colloid* a method to study the free energy barriers for homogeneous nucleation of crystals from a fluid phase, which is not hampered by the fact that the fluid-crystal interface tension in general is anisotropic. By Monte Carlo simulations in the *NpT* ensemble, using the softEAO model for colloidal systems, and by analyzing the equilibrium of a crystal nucleus surrounded by fluid in a small simulation box in thermal equilibrium, the fluid pressure, chemical potential and the volume of the nucleus have been computed to obtain the nucleation barrier. Interesting deviations from the classical nucleation theory with spherical nucleus assumptions have been discovered and analysed.

S. Köhler, F. Schmid and G. Settanni from the University of Mainz investigated in their project *Flexadfg* dynamical properties of fibrinogen and of the initial adsorption stages of fibrinogen on mica and graphite surfaces by atomistic Molecular Dynamics simulations. The adsorption simulations on mica showed a preferred adsorption orientation in a reversible process without large deformations of the protein, and the adsorption simulations on graphite showed an irreversible character and a formation of a large quantity of protein-surface contacts which eventually lead to deformations of the protein and the onset of denaturation.

In the last granting period, quantum mechanical properties of elementary particle systems have been investigated as well as the quantum many body dynamics of trapped bosonic systems.

O.E. Alon, R. Beinke, L.S. Cederbaum, M.J. Edmonds, E. Fasshauer, M.A. Kasevich, S. Klaiman, A.U.J. Lode, N.G. Parker, K. Sakman, M.C. Tsatsos, A.I. Streltsov from the Universities of Haifa (O.E.A.), Heidelberg (R.B., L.S.C., S.K., A.I.S.), Newcastle (M.J.E., N.G.P.), Tromso (E.F.), Stanford (M.A.K.), Basel (A.U.J.L.), Wien (K.S.), Sao Paulo (M.C.T.) studied in their project *MCTDHB* ultracold atomic systems by their method termed multiconfigurational time-dependent Hartree for bosons (MCTDHB). The principal investigators have focused on seven topics: (a) single shots imaging of dynamically created quantum many-body vortices, (b) many-body tunneling dynamics of Bose-Einstein condensates and vortex states in 2D, (c) transition from vortices to solitonic vortices in 2D trapped Bose-Einstein condensates, (d) variance as a sensitive probe of correlations and uncertainty product of an out-of-equilibrium many-particle system, (e) development of a multiconfigurational time-dependent Hartree method for fermions ("MCTDH-X") (f) trapped fermions escape, (g) composite fragmentation of multi-component Bose-Einstein condensates.

C. Alexandrou, K. Jansen, G. Koutsou and C. Urbach from Nicosia (C.A., G.K.), Zeuthen (K.J.) and Bonn (C.U.) investigated in their project GCS-Nops the inner structure of the proton and other hadrons by lattice chromodynamics. By generating the ensemble using directly the physical value of the pion and nucleon masses, the principal investigators were able to compute the hadron spectrum, the axial and tensor charges moments of parton distribution functions and the quark contents of the nucleons.

P. Marquard and M. Steinhauser from Zeuthen (P.M.) and Karlsruhe (M.S.) computed in their project NumFeyn multi-loop Feynman integrals for the electron contribution to the anomalous magnetic moment of the muon, using the FIESTA package.

The Illustris++ Project: The Next Generation of Cosmological Hydrodynamical Simulations of Galaxy Formation

Volker Springel, Annalisa Pillepich, Rainer Weinberger, Rüdiger Pakmor, Lars Hernquist, Dylan Nelson, Shy Genel, Mark Vogelsberger, Federico Marinacci, Jill Naiman, and Paul Torrey

Abstract Cosmological simulations of galaxy formation provide the most powerful technique for calculating the non-linear evolution of cosmic structure formation. This approach starts from initial conditions determined during the Big Bang – which are precisely specified in the cosmological standard model – and evolves them forward in time to the present epoch, thereby providing detailed predictions that test the cosmological paradigm. Here we report first preliminary results from a new

V. Springel (✉)
Astronomisches Recheninstitut, Zentrum für Astronomie der Universität Heidelberg, Mönchhofstr. 12–14, 69120, Heidelberg, Germany

Heidelberg Institute for Theoretical Studies, Schloss-Wolfsbrunnenweg 35, 69118, Heidelberg, Germany
e-mail: volker.springel@h-its.org

A. Pillepich
Max-Planck Institute for Astronomy, Königstuhl 17, 69117, Heidelberg, Germany
e-mail: pillepich@mpia-hd.mpg.de

R. Weinberger • R. Pakmor
Heidelberg Institute for Theoretical Studies, Schloss-Wolfsbrunnenweg 35, 69118, Heidelberg, Germany
e-mail: rainer.weinberger@h-its.org; ruediger.pakmor@h-its.org

L. Hernquist • J. Naiman
Center for Astrophysics, Harvard University, 60 Garden Street, 02138, Cambridge, MA, USA
e-mail: lars.hernquist@cfa.harvard.edu; jill.naiman@cfa.harvard.edu

D. Nelson
Max-Planck Institute for Astrophysics, Karl-Schwarzschild-Str. 1, 85740, Garching, Germany
e-mail: dnelson@mpa-garching.mpg.de

S. Genel
Department of Astronomy, Columbia University, 550 W. 120th St., 10027, New York, NY, USA
e-mail: shygenelastro@gmail.com

M. Vogelsberger • F. Marinacci • P. Torrey
Kavli Institute for Astrophysics and Space Research, MIT, 02139, Cambridge, MA, USA
e-mail: mvogelsb@mit.edu; fmarinac@mit.edu; ptorrey@mit.edu

W.E. Nagel et al. (eds.), *High Performance Computing in Science and Engineering '16*, DOI 10.1007/978-3-319-47066-5_1

generation of hydrodynamical simulations that excel with new physics, enlarged dynamic range and more accurate numerical techniques. The simulations of our ongoing Illustris++ project on HazelHen successfully reproduce the appearance of a red sequence of galaxies that are quenched by accreting supermassive black holes, while at the same time yielding a population of disk galaxies with properties that closely match observational data. Also, we are able to predict the amplification of magnetic fields through small-scale dynamo processes in realistic simulations of large galaxy populations, thereby providing novel predictions for the field strength and topology expected for galaxies of different size and type.

1 Introduction

In principle, simulations of cosmic structure formation are well-specified initial value problems that ought to be able to predict galaxy formation in an ab-initio manner. However, the enormous dynamic range and the complex baryonic processes in galaxy formation make this an extremely challenging multi-scale, multi-physics problem whose full understanding is still a distant goal. Nevertheless, earlier simulations have already proven instrumental for developing our current understanding of structure formation, even given their underlying simplifications. Indeed, cosmological simulations have played a crucial role in establishing ΛCDM as the leading cosmological theory, despite our present ignorance of the true physical nature of dark matter and dark energy.

In particular, dark matter only simulations such as the Millennium simulations [1–3] have led to significant physical insight and reached a high degree of maturity and accuracy. However, such DM-only simulations do not provide predictions regarding the galaxies themselves, and an extra step is required in order to bridge the gap with observations. Primarily two approaches have been used to establish this link: (1) the technique of "semi-analytical modeling", whereby baryonic physics is modeled coarsely at the scale of an entire galaxy and applied in post-processing on top of DM simulations [4, 5], and (2) hydrodynamic simulations, where the evolution of the gaseous component of the Universe is treated using the methods of computational fluid dynamics. The latter approach, together with subgrid prescriptions that provide numerical closure and that take into account astrophysical processes related to star formation, enables the complex interaction of the different baryonic components (gas, stars, black holes) to be treated on a much smaller scale, ideally yielding a self-consistent and powerfully predictive calculation.

Our group has published in 2014 the presently largest hydrodynamic simulations of galaxy formation [6–8]. This simulation suite – dubbed "Illustris" – used a different approach than the ones so far commonly adopted in astrophysics to simulate gas on a computer ("smoothed particle hydrodynamics", SPH, and "Eulerian" mesh-based methods, typically utilizing adaptive mesh refinement, AMR). Illustris employed a moving, unstructured mesh as it has been implemented in our code AREPO [9]: like in AMR, the volume of space is discretized into many individual cells, but as in SPH, these cells move with time, adapting to the flow of gas in their vicinity. As a result, the mesh itself, constructed through a Voronoi tessellation of space, has no preferred directions or regular grid-like structure. Over the past few years, we have shown that this new type of approach for simulating gas has significant advantages over the other two methods, particularly for large cosmological simulations like Illustris [10–13].

One of the major achievements of the Illustris simulation is its ability to track the small-scale evolution of gas and stars within a representative portion of the Universe. The calculation yielded a population of thousands of well-resolved elliptical and spiral galaxies, reproduced the observed radial distribution of galaxies in clusters and the characteristics of hydrogen on large scales, and at the same time it matches the metal and hydrogen content of galaxies on small scales. However, the analysis of Illustris has also revealed a number of tensions with observational data. In particular, it has become clear that the physical model used for the so-called radio-mode feedback [14] of accreting supermassive black holes has been too strong and violent at the scale of galaxy groups and low-mass clusters, causing a depletion of their baryon content. At the same time, this physical model still proved insufficient to quench the central galaxies in these systems to the required degree, causing these galaxies to become too massive. Other problems we identified were the normalization of the faint-end of the galaxy luminosity function, too large galaxy sizes, and a lack of a pronounced bimodality in the galaxy color distribution. In addition, important physical ingredients such as magnetic fields were still missing.

This provides the motivation for the 'Illustris++' project that we currently carry out as a GCS large-scale project on HazelHen at HLRS. The primary scientific goal of our project is to calculate new, unprecedentedly large hydrodynamic simulation models of the universe that improve upon the earlier Illustris project in several important respects. Most importantly, we aim to improve the feedback models by using a newly developed model for black hole accretion and its associated energy release, by employing a considerably improved multi-species chemical enrichment model, by adjusting the treatment of galaxy winds, and last but not least, by adding magnetic fields to our simulations, opening up a rich new area of predictions that are still poorly explored, given that the body of cosmological magneto-hydrodynamic (MHD) simulations is still very small [15–22]. In particular, we aim to study the strength of magnetic field amplification through structure formation as a function of halo and galaxy size. We will also be able to quantify for the first time the expected distribution of magnetic field properties for galaxies of a given size, and to explore the role of winds and strong feedback events in "polluting" the intergalactic-medium with magnetic fields. In addition, we aim for a larger number of resolution elements, and a larger simulation volume than realized previously. This is necessary to study the regime of galaxy clusters better (which are rare and can only be found in a sufficiently large volume), and to allow a sampling of the massive end of the galaxy and black hole mass functions.

At the time of this writing, our project is still running, and only a subset of the production calculations have finished, with some of the main runs presently being computed. In this article, we describe some of the developments undertaken for the project, detail practical and technical aspects of our work, and the status of our runs. We also describe a few preliminary results in an exemplary fashion.

2 Physics and Code Developments for Illustris++

2.1 New Blackhole Physics Model

As discussed above, we replaced the so-called 'radio-mode' of supermassive black hole accretion and feedback in our AREPO code with a novel implementation. The physics of active galactic nuclei (AGN) is crucial for quenching star formation in large galaxies, particularly the central galaxies in groups and clusters of galaxies. While our previous model for blackhole growth in Illustris worked well in certain respects [23], it also showed significant deficits, in particular, it reduced the Sunyaev-Zeldovich decrement in galaxy groups as a result of excessive gas loss, and led to a still insufficient reduction of the star formation rate in the largest clusters, making the central galaxies not red enough.

We have therefore adopted a new kinetic feedback model for AGN driven winds, motivated by recent theoretical suggestions that conjecture advection dominated inflow-outflow solutions for the accretion flows onto the black holes in this regime [24]. For a detailed description of the new model we refer to our recent preprint [25]. In brief, our approach estimates the gas accretion rate through the Bondi-Hoyle-Lyttleton model. However, unlike in previous work, we have eliminated any artificial boost factor to the accretion rate in favor of starting with a slightly higher seed mass of $5 \times 10^5\,\mathrm{M}_\odot$. In terms of feedback, we distinguish between a quasar mode for high accretion rates where the feedback is purely thermal, and a kinetic mode for low accretion rate states where the feedback is purely kinetic. The latter replaces the old radio-mode. Instead, we now inject kinetic energy directly at the position of the black hole, in random directions, so that the time-averaged momentum injection vanishes. The distinction between the two feedback modes is based on the Eddington ratio of the black hole accretion. For Eddington ratios above 0.1, the black hole is assumed to be always in the quasar mode, but for lower Eddington ratios we make the threshold dependent on the black hole mass, such that it becomes progressively easier for low mass black holes to stay in the quasar mode. Or expressed differently, large black hole masses will eventually transition to the kinetic mode, and as this has a higher impact on the host system than the thermal feedback of the quasar mode, this will tend to reduce the accretion rate further, such that the system will then typically stay in the kinetic mode. In the kinetic feedback state, strong quenching of cooling flows and star formation in the halo is possible, such that the corresponding galaxy quickly reddens.

2.2 Hierarchical Time Integration

The simulations carried out in Illustris++ represent a significant challenge not only in terms of size and spatial dynamic range, but also in terms of the dynamic range in timescales. In particular, the strong kinetic AGN feedback, which couples to the densest gas in galaxies, induces very small timesteps for a small fraction of the mass. Over the course of 13 billion years of cosmic evolution, we need up to $\sim 10^7$ timesteps in total. This would be completely infeasible with time integration schemes that employ global timesteps, but even for the individual timestepping we use in AREPO, this represents a formidable problem. It can only be tackled if the computation of sparsely populated timesteps can be made extremely fast so that they do not dominate the total CPU time budget. This in turn requires elimination of overheads that touch the full particle/cell system on such timesteps.

For Illustris++, we have developed a novel hierarchical timestepping scheme in our AREPO code that solves this in a mathematically clean fashion. This is done by recursively splitting the Hamiltonian describing the dynamics into a ‘slow’ and a ‘fast’ system (similar to [26]). One important feature of this time integration scheme is that the split-off fast system is self-contained, i.e. its evolution does not rely on any residual coupling with the “slow” part. This means that our goal, namely that poorly populated short timesteps can be computed without touching any parts of the system living on longer timesteps, can be realized.

2.3 Chemical Enrichment Model

For Illustris++, we have also improved our modelling of chemical enrichment, both by using updated yield tables that account for the most recent results of stellar evolution calculations, and by making the tracking of different chemical elements more accurate and informative. The most important technical measure to achieve this has been the introduction of a fiducial “other chemical elements” mass bin, such that together with the explicit tracking of 9 chemical elements (H, He, C, N, O, Ne, Mg, Si, Fe), the metal abundance vector accounts for the full mass content of every cell or star. Since we do a spatial reconstruction for every element individually, the previous code could arrive at extrapolated flux vectors at cell interfaces with an unphysical sum of the 9 explicitly tracked elements, leaving for the other elements a negative contribution. In our new treatment, the density of these other elements is reconstructed as well, and the abundance pattern is renormalized after extrapolation, thereby always leading to physically viable chemical compositions at flux exchanges.

The other significant change we made is that we now account with special chemical tagging fields separately for metals produced by asymptotic giant branch (AGB) stars, type-II supernovae, and type-Ia supernovae. This has not been done before in such hydrodynamical simulations, and opens up a rich additional set of analysis possibilities which are largely unexplored thus far. Given that the metallicity patterns in the circumgalactic medium are emerging as a critical observational diagnostic and constraint for the feedback physics, this is a very timely extension of our modelling capabilities.

2.4 Hydrodynamical Accuracy Improvements

For certain problems, the original implementation of AREPO reached only first-order convergence in the L_1 norm. In [27] we have shown that this can be rectified by simple modifications in the time integration scheme and the spatial gradient estimates of the code, both acting together to improve the accuracy of the code. As a result, the new formulation used for Illustris++ is now second-order accurate under the L_1 norm even in unfavorable situations. As a welcome side effect, conservation of angular momentum is substantially improved, too. We have found that these changes can significantly improve the results of smooth test problems. On the other hand, we also showed that cosmological simulations of galaxy formation are unaffected for well resolved galaxies, demonstrating that the numerical errors eliminated by the new formulation do not impact these simulations significantly. Nevertheless, the improved accuracy of the new formulation is clearly to be preferred, and we expect that small, poorly resolved galaxies are rendered more accurately in Illustris++ than before, corroborating the advantage of our moving-mesh technique compared to SPH or AMR codes in this regime.

We have also made important improvements to the ideal magnetodynamics (MHD) solver in our code [28], primarily in the form of an additional timestep criterion that controls the size of the Powell source terms applied for divergence control. Previously, this was not checked explicitly, instead the timestep of a cell was determined only by the Courant condition and a kinematical timestep constraint. It could thus happen under rare conditions that the source terms would apply order unity corrections to the magnetic field over the course of a timestep, leading to a relatively large local error. In our new code used for Illustris++, this is now safely prevented, increasing both the accuracy and robustness of our MHD implementation.

2.5 Elimination of All-to-All Communication Steps

In the AREPO code, we need to carry out, at multiple places, parallel, distributed tree walks that serve to calculate, e.g., the short-range gravitational field, the local enrichment region of stellar populations, or the zone of accretion around a supermassive black hole. Algorithmically, each MPI rank first does a range-search on its local domain, during which it also detects if the search region overlaps with other domains. In the latter case, a search request to the foreign domain is registered. These are exchanged to the corresponding target rank and processed in a second phase of the distributed tree walk. The number of these search requests for each of the other possible MPI ranks is stored in a table. After the first tree walk phase, the table is communicated with an MPI_Alltoall such that each rank knows how many items it needs to import from each other processor. As the domain layout is highly irregular as a result of the work-load and memory-balancing, the detailed communication pattern arising here is irregular and sparse, and cannot be predicted ahead of time.

The sparseness however implies that for a large number of MPI ranks mostly zero entries are communicated in the MPI_Alltoall. This has not been a critical source of overhead thus far if the dynamic range of the simulation is limited, but becomes an issue in simulations with 10^4 MPI ranks and beyond, where the smallest timesteps (which are carried out most frequently) need to be very fast so as to not start dominating the total CPU budget. Illustris++ runs on HazelHen are our first large production simulations where this source of overhead plays a sizable role.

To mitigate this, we have developed during the first project phase a relatively involved rewrite of our communication patterns in the parallel tree walks, which can completely eliminate the need for an MPI_Alltoall. Instead, we can now employ a sparse communication pattern that makes use of an asynchronous collective barrier. The latter is in principle available as part of MPI-3.0, but for compatibility reasons with older systems that do not yet support MPI-3.0 we have implemented an efficient sparse asynchronous communication pattern for the distributed tree walks ourselves, relying only on MPI-2 features.

3 Simulation Set and Production Runs

After obtaining access to HORNET/HazelHen, we have first carried out a limited number of test simulations plus a number of science runs of zooms into the Illustris volume targeting individual galaxies (these also served to test our new physics implementations, and several publications about them are currently in preparation). These had confirmed that our simulation code AREPO runs effectively and without technical issues on the new Cray XC40 machine. This also helped us to establish the precise performance for our simulation work-load, both with respect to computational throughput, communication bandwidth and I/O speed. In all three areas, the high expectations we had for the XC40 were met (module some I/O issues that initially surfaced, but which could be resolved by switching our project to a different filesystem). Also, our tests did not reveal any technical obstacles against carrying out our simulations, aside from a surprisingly low memory ceiling for the application code on the compute nodes. We could initially not use more than ∼3900 MB per core in large partition runs without sometimes falling victim to OOMs, caused by memory needs of the I/O subsystem and MPI buffers. How to work around this reliably required a lot of experimenting and testing on our end.

After finalizing our modification of the physical model of Illustris++, we adjusted our plans for the primary science runs in the project by first carrying out "IllustrisPrime", a very demanding simulation with 18 billion resolution elements in a $75\,h^{-1}$Mpc box similar to the original Illustris run, but now using the new full physics model of Illustris++ with all its improvements, as well as including magneto-hydrodynamics (MHD). We also now adopted the newest cosmological models as determined by the PLANCK Satellite. This cosmological simulation is the first that includes MHD and resolves galaxy formation at high resolution, opening up many possibilities for novel predictions. Also, IllustrisPrime will be ideal to convincingly demonstrate that we can solve the problems at the bright end of the galaxy luminosity functions that have troubled all previous simulations in the field, including our older Illustris simulation that presently defines the state-of-the-art in this area.

In Table 1, we give an overview of our primary production simulations, omitting smaller test calculations. We are currently still in the process of finalizing one of

Table 1 Overview of primary production runs carried out by the Illustris++ project. All simulations use PLANCK cosmological parameters and are carried out with a tracer particle method that is faithful with respect to the mass flux in the system between all baryonic components. We typically use two Monte Carlo tracers per Voronoi cell, i.e. $N_{\rm tracers} = 2 \times N_{\rm cells}$. All simulations follow more than 13 billion years of cosmic evolution, with smallest timesteps of order a few thousand years

Symbolic name	Boxsize	$N_{\rm dm}$	$N_{\rm cells}$	MPI ranks	Physics	Run status
L75n1820TNG	$75\,h^{-1}$Mpc	1820^3	1820^3	10,752	Final full physics model	Advanced
L75n1820MF	$75\,h^{-1}$Mpc	1820^3	1820^3	12,000	Alternative AGN feedback	Finished
L75n910TNG	$75\,h^{-1}$Mpc	910^3	910^3	2688	Final full physics model	Finished
L75n455TNG	$75\,h^{-1}$Mpc	455^3	455^3	336	Final full physics model	Finished
L205n2500TNG	$205\,h^{-1}$Mpc	2500^3	2500^3	24,000	Final full physics model	Started
L35n2160TNG	$35\,h^{-1}$Mpc	2160^3	2160^3	16,320	Final full physics model	Started
L25n512TNG	$25\,h^{-1}$Mpc	512^3	512^3	1200	Final full physics model	Finished
L12.5n512TNG	$12.5\,h^{-1}$Mpc	512^3	512^3	1200	Final full physics model	Finished

our main production runs using 10,752 cores on HazelHen, while IllustrisPrime has already finished. In addition, we are carrying out two further large calculations which just have been started. They are substantially larger and either excel in volume or mass resolution, respectively. We have already transferred more than 240 TB of production data to the Heidelberg Institute of Theoretical Studies, in part by using fast gridftp services offered by HLRS. From the ongoing runs, we expect about 200 TB of additional data, which we will also transfer to Heidelberg for the scientific analysis in the coming years.

4 Selected Preliminary Results

In Fig. 1, we illustrate the large-scale distribution of different quantities in the IllustrisPrime simulation (L75n1820MF). From top to bottom, we show projections of the gas density field, the mean mass-weighted metallicity, the mean magnetic field strength (field energy weighted), the dark matter density, and the stellar density. The displayed regions are 75 h^{-1}Mpc from left to right, and 3.75 h^{-1}Mpc deep. We can nicely see the cosmic web on large-scales, formed both in the dark matter and the diffuse gas. The color hue in the gas distribution shown on top encodes the mass-weighted temperature across the slice. We see that the largest halos are filled with hot plasma, and in addition, there is clearly evidence for very strong outflows in the largest halos impinging on the intergalactic medium, leading to relatively widespread heating.

The bottom panel in Fig. 1 displays the stellar mass density. Clearly, on the scales shown in this image, the individual galaxies appear as very small dots, illustrating that the stellar component fills only a tiny fraction of the volume. However, our simulations have enough resolution and dynamic range to actually resolve the internal structure of these galaxies in remarkable detail. This is shown in Fig. 2, which zooms in on two disk galaxies formed in our simulations. The one on the right hand panel is in a more massive halo and has a more massive black hole. This in fact has made it start to transition into the quenched regime, which here begins by a reduced star formation in the center as a result of kinetic AGN feedback. The outskirts of the galaxy still support some level of star formation, causing blue spiral arms.

Of particular interest in our new simulations is the magnetic field that builds up in halos and galaxies. In Fig. 3, we show a typical disk galaxy in a face-on orientation, plotting the magnetic vector field overlaid on a rendering of the gas density in the background. We see that the field is ordered in the plane of the disk, where it has been amplified by shearing motions to sizable strength. Interestingly, there are multiple field reversals and a complicated topology of the field surrounding the disk. The magnetic field not only provides additional pressure for the gas, but also is of critical importance for transport processes of heat energy and cosmic rays. Our realistic field topologies should be very useful for studying the propagation of

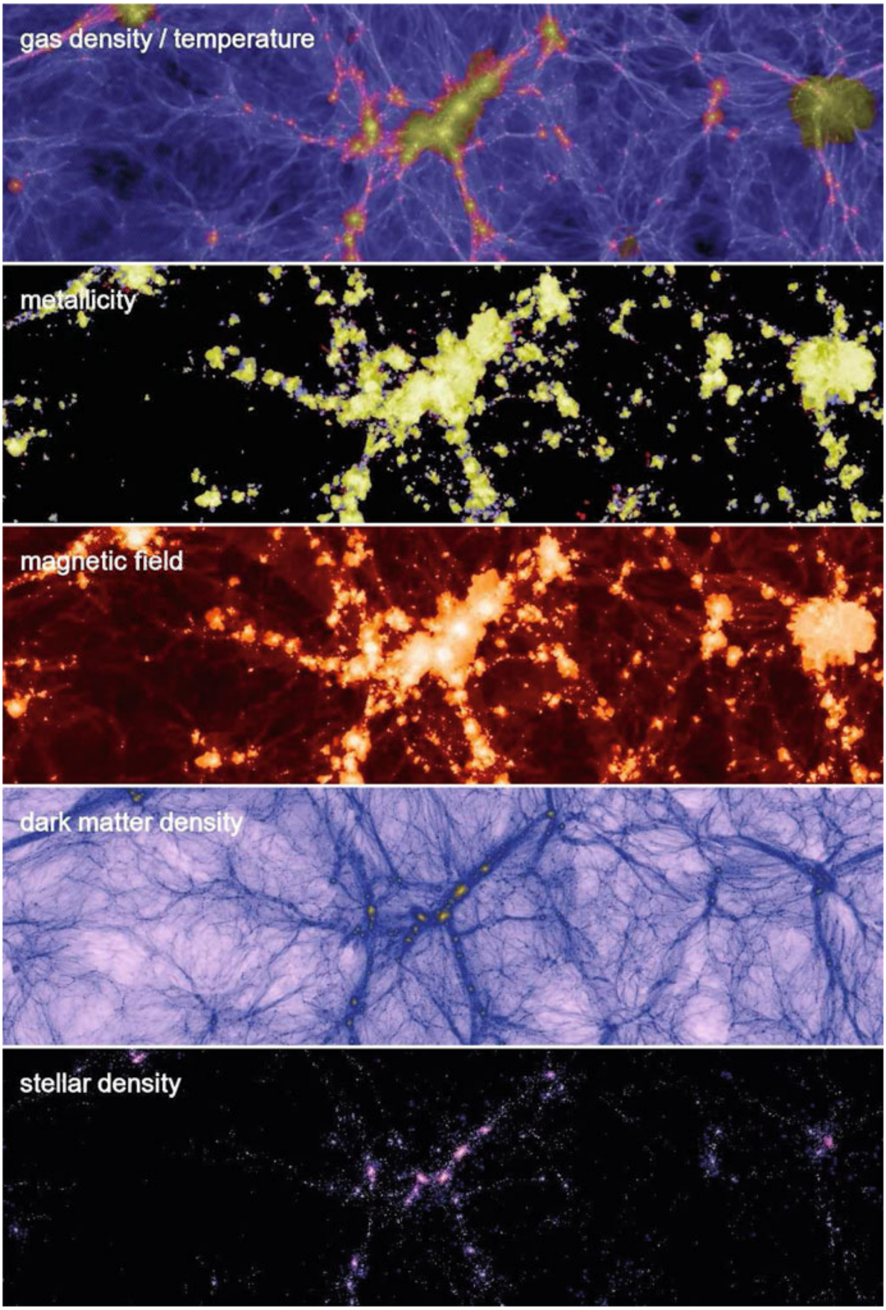

Fig. 1 Thin projections through the L75n1820MF simulation, showing the gas density field, the metallicity, the magnetic field strength, the dark matter density, and the stellar density

Fig. 2 Stellar mass distributions of two disk galaxies in halos of mass $8.3 \times 10^{11}\,M_\odot$ (*left*) and $2.0 \times 10^{12}\,M_\odot$ (*right*), respectively, in face-on (*top*) and edge-on projections (*bottom*). The stellar colors are assigned according to their age and metallicity

cosmic rays in the Milky Way, and for analyzing the deflections of ultra-high energy cosmic rays of extra-galactic origin.

In Fig. 4, we show an analysis of the typical magnetic field strengths reached in halos of different size. We here plot radial profiles for four different halo masses, stacking up to 50 halos in a narrow mass range around the virial masses 10^{10}, 10^{11}, 10^{12}, and $10^{13}\,M_\odot$. We see that field strengths of several μG are reached in the centres of galaxies in halos of masses $10^{11} - 10^{12}\,M_\odot$, in good agreement with typical observed fields. In smaller halos, the fields are still notably weaker, presumably because here they have not yet been amplified as efficiently. In larger halos, $10^{13}\,M_\odot$ and beyond, they are also weaker in the centers, but for a different reason. Here some of the magnetic flux is expelled by strong nuclear outflows driven by AGN feedback. In any case, the strength of the simulated fields implies a remarkable amplification relative to the primordial fields that we seeded in the initial conditions. This initial field strength is empirically largely unconstrained, but our results reached for the field strength in galactic centres do not depend on the value we used (which in our case was 10^{-11} Gauss) over a wide dynamic range, because the magnetic amplification processes stop once the dynamo processes responsible for the exponential amplification saturate. This happens when the magnetic pressure becomes comparable to the thermal pressure.

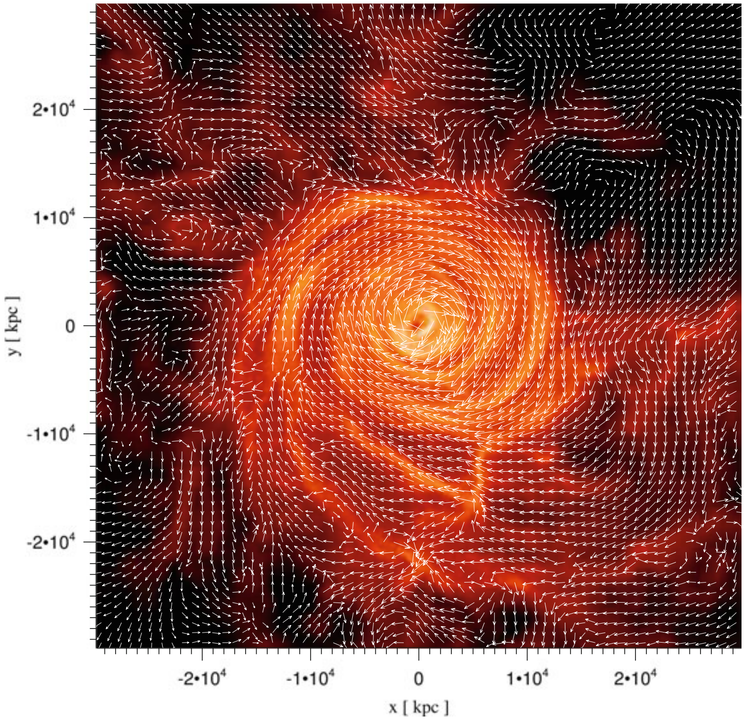

Fig. 3 Magnetic field structure in a disk galaxy (the one displayed in the left-hand panel of Fig. 2), overlaid over a rendering of the gas density structure (color-scale in the background). The length of the drawn vectors is made only weakly dependent on the magnetic field strength (as $\propto |\mathbf{B}|^{1/4}$) in order to see more of the field structure in the regions with weaker fields

On large scales, however, the magnetic field strengths reached in voids still reflect the initial field. This is clearly seen in Fig. 5, which gives a phase-space diagram of gas density versus magnetic field strength. The correlation $B \propto \rho^{2/3}$ (indicated as a solid line) reflects adiabatic expansion/compression of the initial field set at the starting redshift $z = 127$. At baryonic overdensities of around 100, we see that much larger fields are created. This is in part due to the amplification of the field through large-scale shearing flows and in part due to a small-scale dynamo driven by star formation and galactic wind feedback on small scales.

In sum, our calculations demonstrate that already an extremely tiny magnetic field left behind by the Big Bang is sufficient to explain orders of magnitude larger field strengths observed today. Interestingly, the magnetic field strength found in the simulation agrees very well with the values measured for the Milky Way and neighboring galaxies. This is remarkable given that there are no free parameters influencing the magnetic field amplification that could be tuned to modify the final field strength reached in our simulated galaxies.

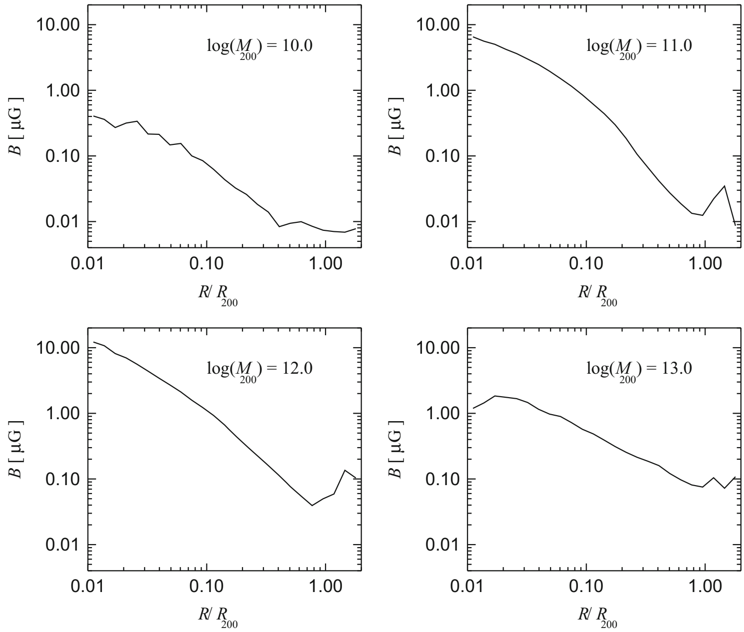

Fig. 4 Spherically averaged profiles of the mean magnetic field strength in halos of different mass. Each panel shows a stacked set of up to 50 halos in a narrow mass bin around a different virial mass, as labeled in each panel

Another powerful application of our simulations lies in studies of the metal enrichment in the universe. We track 9 chemical elements explicitly, and all other elements are lumped together in a 10-th fiducial component so that the advected metallicity vectors always correspond to physically meaningful abundance patterns in all situations. In addition, we use a newly developed metal tagging technique, allowing us to characterize which fraction of metals in every cell or star originated from AGB stars, supernova type II explosions, or type-Ia explosions.

In Fig. 6, we show a break down of the total metal content in the gas phase of the simulated universe at different times as a function of gas density. The individual histograms are normalized to the total metal content in the gas at the corresponding epoch. The distributions can hence answer the question at which gas densities the majority of the metals can be found. Interestingly, we see that most of the metals are actually stored at gas densities that correspond to the circumgalactic medium, whereas only a smaller fraction is contained in the star-forming interstellar medium, and very little in the low-density intergalactic medium. The relative shares between these phases are time-dependent, with more metals found in low density gas towards late times. This is most likely a result of the feedback that expelled these metals from the galaxies.

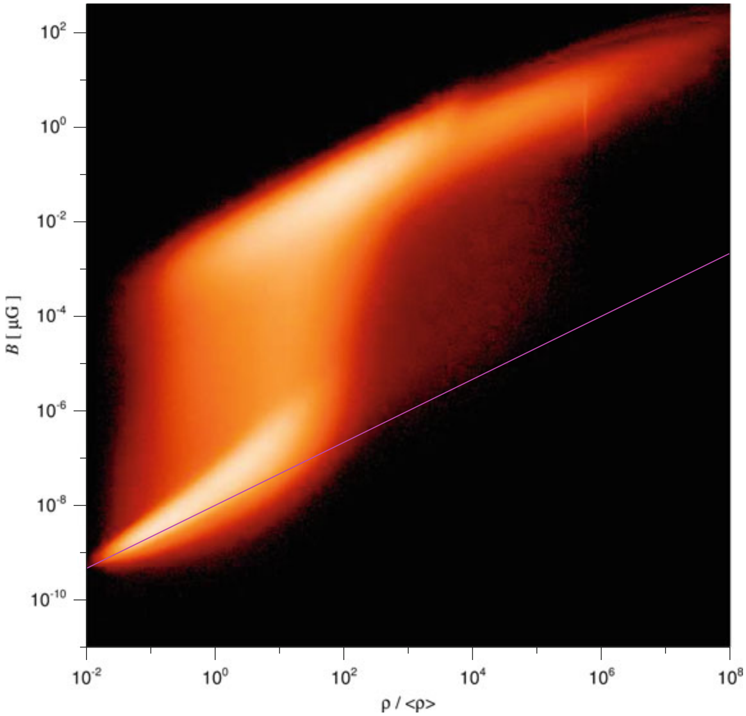

Fig. 5 Phase-space diagram of the magnetic field strength versus gas overdensity at $z = 0$ in one of our Illustris++ simulations. The *line* shows the locus corresponding to adiabatic compression or expansion of the initial field strength

5 Conclusions

Understanding the feedback processes in galaxy formation and evolution is the principal challenge in theoretical extragalactic astronomy. This question is also of critical relevance for cosmology, as baryonic processes impact the distribution of dark matter, and hence in turn affect cosmological probes that aim to constrain, for example, the physical properties of dark energy. Solving the feedback conundrum is unthinkable without further refining the simulation models and the employed numerical methods. This is due to the multi-scale and multi-physics nature of the problem, which tends to limit analytic approaches for studying the problem to highly schematic and correspondingly uncertain models.

The Illustris++ project aims to redefine the state-of-the-art of cosmological hydrodynamical simulations of galaxy formation. In particular, our new simulations make significant progress on predicting the bright end of the galaxy luminosity function through the use of a new model for AGN feedback. Also, realistic galaxy sizes, morphologies and colors are obtained at the same time. The scientific analysis of the simulation promises a rich harvest and will primarily focus on testing the

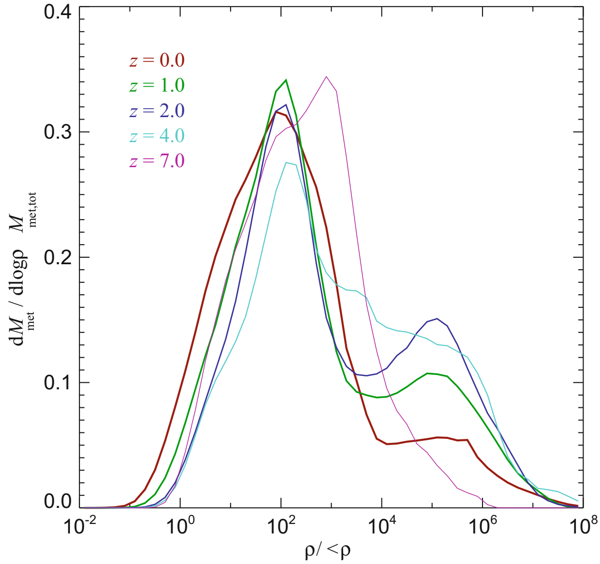

Fig. 6 Distribution of the gas phase metal content with respect to baryonic overdensity at different epochs, as labelled. Each distribution is normalized to the total metal mass in the gas at the corresponding time

models further. Our simulation predictions for the gas around galaxies, the so-called circum-galactic medium (CGM) are particular timely, as the Cosmic Origins Spectrograph (COS) on board of the Hubble Space Telescope (HST) has provided a wealth of absorption line data probing this phase. In addition, our simulations allow us to make novel, testable predictions for the magnetic field strength in different environments, and its correlation with other galaxy properties.

Acknowledgements The authors gratefully acknowledge computer time through the project GCS-ILLU on Hornet/HazelHen at HLRS. We acknowledge financial support through subproject EXAMAG of the Priority Programme 1648 'SPPEXA' of the German Science Foundation, and through the European Research Council through ERC-StG grant EXAGAL-308037, and we would like to thank the Klaus Tschira Foundation.

References

1. Springel, V., White, S.D.M., Jenkins, A., Frenk, C.S., Yoshida, N., Gao, L., Navarro, J., Thacker, R., Croton, D., Helly, J., Peacock, J.A., Cole, S., Thomas, P., Couchman, H., Evrard, A., Colberg, J., Pearce, F.: Nature **435**, 629 (2005). doi:10.1038/nature03597
2. Boylan-Kolchin, M., Springel, V., White, S.D.M., Jenkins, A., Lemson, G.: MNRAS **398**, 1150 (2009). doi:10.1111/j.1365-2966.2009.15191.x
3. Angulo, R.E., Springel, V., White, S.D.M., Jenkins, A., Baugh, C.M., Frenk, C.S.: MNRAS **426**, 2046 (2012). doi:10.1111/j.1365-2966.2012.21830.x

4. Kauffmann, G., Colberg, J.M., Diaferio, A., White, S.D.M.: MNRAS **303**, 188 (1999). doi:10.1046/j.1365-8711.1999.02202.x
5. Cole, S., Lacey, C.G., Baugh, C.M., Frenk, C.S.: MNRAS **319**, 168 (2000). doi:10.1046/j.1365-8711.2000.03879.x
6. Vogelsberger, M., Genel, S., Springel, V., Torrey, P., Sijacki, D., Xu, D., Snyder, G., Bird, S., Nelson, D., Hernquist, L.: Nature **509**, 177 (2014). doi:10.1038/nature13316
7. Vogelsberger, M., Genel, S., Springel, V., Torrey, P., Sijacki, D., Xu, D., Snyder, G., Nelson, D., Hernquist, L.: MNRAS **444**, 1518 (2014). doi:10.1093/mnras/stu1536
8. Genel, S., Vogelsberger, M., Springel, V., Sijacki, D., Nelson, D., Snyder, G., Rodriguez-Gomez, V., Torrey, P., Hernquist, L.: MNRAS **445**, 175 (2014). doi:10.1093/mnras/stu1654
9. Springel, V.: MNRAS **401**, 791 (2010). doi:10.1111/j.1365-2966.2009.15715.x
10. Vogelsberger, M., Sijacki, D., Kereš, D., Springel, V., Hernquist, L.: MNRAS **425**, 3024 (2012). doi:10.1111/j.1365-2966.2012.21590.x
11. Sijacki, D., Vogelsberger, M., Kereš, D., Springel, V., Hernquist, L.: MNRAS **424**, 2999 (2012). doi:10.1111/j.1365-2966.2012.21466.x
12. Torrey, P., Vogelsberger, M., Sijacki, D., Springel, V., Hernquist, L.: MNRAS **427**, 2224 (2012). doi:10.1111/j.1365-2966.2012.22082.x
13. Bauer, A., Springel, V.: MNRAS **423**, 2558 (2012). doi:10.1111/j.1365-2966.2012.21058.x
14. Sijacki, D., Springel, V., Di Matteo, T., Hernquist, L.: MNRAS **380**, 877 (2007). doi:10.1111/j.1365-2966.2007.12153.x
15. Dolag, K., Bartelmann, M., Lesch, M.: A&A **348**, 351 (1999)
16. Dolag, K., Bartelmann, M., Lesch, H.: A&A **387**, 383 (2002). doi:10.1051/0004-6361:20020241
17. Dolag, K., Grasso, D., Springel, V., Tkachev, I.: J. Cosmol. Astropart. Phys. **1**, 009 (2005). doi:10.1088/1475-7516/2005/01/009
18. Donnert, J., Dolag, K., Lesch, H., Müller, E.: MNRAS **392**, 1008 (2009). doi:10.1111/j.1365-2966.2008.14132.x
19. Bonafede, A., Dolag, K., Stasyszyn, F., Murante, G., Borgani, S.: MNRAS **418**, 2234 (2011). doi:10.1111/j.1365-2966.2011.19523.x
20. Kotarba, H., Lesch, H., Dolag, K., Naab, T., Johansson, P.H., Donnert, J., Stasyszyn, F.A.: MNRAS **415**, 3189 (2011). doi:10.1111/j.1365-2966.2011.18932.x
21. Beck, A.M., Lesch, H., Dolag, K., Kotarba, H., Geng, A., Stasyszyn, F.A.: MNRAS **422**, 2152 (2012). doi:10.1111/j.1365-2966.2012.20759.x
22. Marinacci, F., Vogelsberger, M., Mocz, P., Pakmor, R.: MNRAS **453**, 3999 (2015). doi:10.1093/mnras/stv1692
23. Sijacki, D., Vogelsberger, M., Genel, S., Springel, V., Torrey, P., Snyder, G.F., Nelson, D., Hernquist, L.: MNRAS **452**, 575 (2015). doi:10.1093/mnras/stv1340
24. Yuan, F., Narayan, R.: ARA&A **52**, 529 (2014). doi:10.1146/annurev-astro-082812-141003
25. Weinberger, R., Springel, V., Hernquist, L., Pillepich, A., Marinacci, F., Pakmor, R., Nelson, D., Genel, S., Vogelsberger, M., Naiman, J., Torrey, P.: ArXiv e-prints (2016)
26. Pelupessy, F.I., Jänes, J., Portegies Zwart, S.: New A **17**, 711 (2012). doi:10.1016/j.newast.2012.05.009
27. Pakmor, R., Springel, V., Bauer, A., Mocz, P., Munoz, D.J., Ohlmann, S.T., Schaal, K., Zhu, C.: MNRAS **455**, 1134 (2016). doi:10.1093/mnras/stv2380
28. Pakmor, R., Bauer, A., Springel, V.: MNRAS **418**, 1392 (2011). doi:10.1111/j.1365-2966.2011.19591.x

Hydrangea: Simulating a Representative Population of Massive Galaxy Clusters

Yannick M. Bahé, for the C-EAGLE collaboration

Abstract Galaxy clusters are the most massive bound structures in the Universe, and contain not only up to several thousand galaxies, but also extended haloes of dark matter and hot gas. Observations show that galaxies in clusters differ from those living in more isolated parts of the Universe, but the physics of how clusters shape their galaxies is at present not well understood. Not only does this constitute a major gap in our understanding of galaxy formation, but it also limits the use of galaxy clusters as cosmological probes. In the *Hydrangea* project, we have created a suite of 24 simulated galaxy clusters at unprecedented resolution, using a state of the art galaxy formation model developed for the EAGLE project. Detailed scientific analysis of the simulation outputs, which has only just begun, is expected to lead to major new insight into the physics of both galaxy formation in an extreme environment and the growth of the massive haloes in which cluster galaxies are embedded.

1 Introduction

Galaxy clusters are collections of large numbers of galaxies – up to several thousands in the most extreme cases – occupying a region in our Universe that is typically a few megaparsec (Mpc[1]) in size. Moreover, observations have firmly established that the galaxies which are seen in optical light are in fact only a minor component of these objects: the dominant constituents in terms of mass are instead extended, diffuse 'haloes' of dark matter (DM) and very hot gas (the 'intra-cluster medium' or ICM) that together account for typically more than 90 % of the mass of a galaxy cluster [1]. Including these optically invisible components, the mass of the largest such objects exceeds 10^{15} times the mass of our Sun ($M_{\odot}$), making

[1]The *parsec* (pc) is the standard unit of length in astronomy, with $1\,\text{pc} = 3.08 \times 10^{16}$ m.

Y.M. Bahé (✉)
Max Planck Institut für Astrophysik, Karl-Schwarzschild-Str. 1, 85748, Garching, Germany
e-mail: ybahe@mpa-garching.mpg.de

W.E. Nagel et al. (eds.), *High Performance Computing in Science and Engineering '16*, DOI 10.1007/978-3-319-47066-5_2